# Podocyte-Derived Vascular Endothelial Growth Factor Mediates the Stimulation of α3(IV) Collagen Production by Transforming Growth Factor-β1 in Mouse Podocytes

**Sheldon Chen, Yuki Kasama, Joseph S. Lee, Belinda Jim, Maria Marin, and Fuad N. Ziyadeh**

**Podocyte-derived vascular endothelial growth factor (VEGF) is upregulated in diabetes and may contribute to albuminuria. Although believed to act upon the glomerular endothelium, VEGF may have pronounced effects on the podocyte itself. The functionality of this VEGF autocrine loop was investigated in conditionally immortalized mouse podocytes. Exogenous VEGF$_{164}$ increased the production of α3(IV) collagen, an integral component of the glomerular basement membrane (GBM); this effect was completely prevented by SU5416, a pan-VEGF receptor inhibitor. The VEGF inhibitor also partially prevented the stimulation of α3(IV) collagen by transforming growth factor (TGF)-β1, establishing a novel role for endogenous VEGF. However, VEGF did not influence the production of another novel chain of collagen IV, α5(IV) collagen, and SU5416 failed to reverse the known inhibitory effect of TGF-β1 on α5(IV) collagen production. Cultured mouse podocytes possess at least the VEGFR-1 receptor, confirmed by RT-PCR, immunoblotting, and immunocytochemistry. By these techniques, however, VEGFR-2 is absent. VEGF signaling proceeds via autophosphorylation of VEGFR-1 and activation of the phosphatidylinositol 3-kinase (PI3K) pathway. Thus, podocyte-derived VEGF operates in an autocrine loop, likely through VEGFR-1 and PI3K, to stimulate α3(IV) collagen production. The TGF-β1–stimulated endogenous VEGF may have significant implications for podocyte dysfunction in diabetic glomerulopathy, manifesting as GBM thickening and altered macromolecular permeability.** *Diabetes* **53: 2939–2949, 2004**

V ascular endothelial growth factor (VEGF) functions to induce angiogenesis (1) and increase microvascular permeability (2), as implied by its original name, vascular permeability factor (3). While its angiogenic property is not evident in the adult kidney (4), its permeabilizing effect has been implicated in the proteinuria of diabetic nephropathy where VEGF levels are increased (5,6), and anti-VEGF therapy partially prevents albuminuria in type 1 and type 2 diabetic rodents (7,8). The major source of VEGF in the glomerulus is the visceral epithelial cell, or podocyte, which produces VEGF in a constitutive manner (9). The function of podocyte-derived VEGF is currently unknown, but it is thought to act across the glomerular basement membrane (GBM) upon the glomerular endothelial cell (7,10,11). This scenario, however, requires that VEGF be transported against the flow of glomerular filtration (12).

Alternatively, the podocyte-produced VEGF may act upon the podocyte itself in an autocrine loop via the activation of VEGF signaling receptors (10,11). The three major VEGF receptors are termed VEGFR-1 (or Flt-1), VEGFR-2 (or Flk-1/KDR), and VEGFR-3 (or Flt-4) (13). An additional ancillary receptor called neuropilin-1 (or VEGF$_{164}$R) enhances the binding of VEGF$_{164}$ to VEGFR-2 (14). In human podocytes, VEGFR-1 and -3 and neuropilin-1 have been identified at the mRNA level only, but the message for VEGFR-2 appears to be absent (10). In general, the VEGF receptors signal via their tyrosine kinase activities. Specific inhibitors of these receptor kinases have been used to block VEGF signaling and have proved invaluable in establishing a role for VEGF in disease pathophysiology (15,16). One such inhibitor is SU5416 (SUGEN/Pfizer), a small molecule that selectively blocks all of the VEGF receptor kinases (15).

Downstream of the VEGF receptors, the signaling cascade can continue through one of several protein kinase pathways (17). For instance, the phosphatidylinositol 3-kinase (PI3K)-Akt pathway has been shown to mediate the growth effects of VEGF in proximal tubular cells (6). An inhibitor of PI3K, LY294002 (Eli Lilly, Indianapolis, IN), has been used to show that the PI3K-Akt pathway mediates such VEGF effects as angiogenesis, cell survival, and increased vascular permeability (18–20). Based on these considerations, we used SU5416 and LY294002 to counteract endogenous VEGF and to substantiate the functionality of a VEGF autocrine system in cultured podocytes.

Endogenous VEGF production in kidney cells can be stimulated by a number of pathophysiologic features of the diabetic state, such as high glucose, angiotensin II, protein kinase C, and cellular stretch (21–23). One of the most effective means, however, is treatment with the

cytokine, transforming growth factor (TGF)-β1, which augments VEGF secretion by over twofold in cultured podocytes (21). We had also previously shown that TGF-β1 stimulates production of the α3 chain of type IV collagen (21) but inhibits the level of the α5(IV) chain, both principal constituents of the GBM meshwork. Therefore, the effects of TGF-β1 on type IV collagen can be mediated, at least in part, by the autocrine VEGF system in podocytes (24).

The GBM is an important part of the glomerular filtration barrier to macromolecules. In this context, the investigation of type IV collagen is highly relevant to the study of diabetic nephropathy in which the GBM is diffusely thickened (25,26) but somehow more porous to the passage of albumin (27). This paradox could be related to an abnormal buildup or disrupted assembly of certain type IV collagen chains and other matrix proteins, resulting in thickening of the GBM (28,29) while at the same time perturbing its barrier function (30). Since the glomerular α3(IV) and α5(IV) chains are both produced by the podocyte, we sought to determine whether the podocyte's endogenous VEGF system may play a role in the dysregulation of these collagen proteins.

## RESEARCH DESIGN AND METHODS

**Podocyte cell culture.** Conditionally immortalized mouse podocytes were kindly provided by Dr. Peter Mundel (Albert Einstein College of Medicine, Bronx, NY) and were handled as previously described (21). The cells harbor a temperature-sensitive variant of the SV40 large T antigen (tsA58) that is inducible by γ-interferon and stable at 33°C but rapidly degraded at 37–39°C (31). At 33°C, the large T antigen allows for cellular proliferation. The growing cells are maintained in collagen I–coated flasks in RPMI-1640 media supplemented with 10% FCS, 100 units/ml penicillin, 100 μg/ml streptomycin, and 10 units/ml mouse recombinant γ-interferon. When the cells have reached confluence, they are passaged and allowed to differentiate at 37.5°C for 2 weeks without γ-interferon in Dulbecco's modified Eagle's medium containing 5.5 mmol/l glucose, 5% FCS, 100 units/ml penicillin, and 100 μg/ml streptomycin. Podocyte differentiation is evidenced by the expression of α-synaptopodin (31).

**Experimental treatment conditions.** Differentiated podocytes were treated with exogenous recombinant mouse $VEGF_{164}$ (R&D Systems, Minneapolis, MN) in concentrations of 2, 8, and 20 ng/ml for 24 or 48 h. Recombinant human TGF-β1 (R&D Systems) was added at 2 ng/ml for 48 h. This dose and duration has been shown to significantly stimulate endogenous VEGF secretion and α3(IV) collagen production as well as inhibit α5(IV) collagen production in mouse podocytes (21). Concurrent with the VEGF or TGF-β1 treatment, the following specific inhibitors were added in certain experiments: a pan-VEGF receptor inhibitor (SU5416; gift of SUGEN/Pfizer; $IC_{50}$ [half-maximal inhibitory concentration] ~1 μmol/l for inhibition of receptor autophosphorylation) (32), a PI3K inhibitor (LY294002; Calbiochem, San Diego, CA), or a TGF-β1 receptor kinase inhibitor (SB-431542; GlaxoSmithKline, King of Prussia, PA) (21,33).

**Western immunoblotting.** Preparation of total lysate protein in radioimmunoprecipitation assay buffer followed by SDS-PAGE (3–8 or 4–12% gradient; NuPAGE precast gels; Invitrogen, Carlsbad, CA) and wet transfer to a nitrocellulose membrane (Bio-Rad, Hercules, CA) were performed as previously described (21). The membrane was blocked in 5% nonfat milk in Tris-buffered saline/0.1% Tween 20 and probed overnight at 4°C with one of the following primary antibodies: human anti–α3(IV) collagen (gift of Dr. Michael Madaio, University of Pennsylvania), rabbit anti–α5(IV) collagen (gift of Dr. Jean-Francois Beaulieu, University of Sherbrooke, Québec, Canada), rabbit anti–VEGFR-1 (NeoMarkers/LabVision, Fremont, CA), rabbit anti–VEGFR-2 (NeoMarkers), rabbit anti–phospho-VEGFR-1 (Oncogene Research Products, San Diego, CA), rabbit anti-Smad2 (Zymed, South San Francisco, CA), rabbit anti–phospho-Smad2 (Upstate Biotechnology, Charlottesville, VA), or mouse anti–β-actin antibody (Sigma, St. Louis, MO). In some cases, the blocking peptide for VEGFR-1 and -2 (both NeoMarkers) or clusterin (Santa Cruz Biotechnology, Santa Cruz, CA) was incubated overnight with the corresponding antibody before use. After three washes in Tris-buffered saline/0.1% Tween 20, membranes were probed with a secondary goat anti-human (Jackson ImmunoResearch, West Grove, PA), donkey anti-rabbit

(Amersham Biosciences, Piscataway, NJ), or sheep anti-mouse antibody (Amersham), each conjugated to horseradish peroxidase (HRP). The HRP-catalyzed chemiluminescence reaction was developed with SuperSignal West Pico substrate (Pierce Biotechnology, Rockford, IL), allowing the detection of immunoreactive protein bands. The membrane was reprobed with β-actin to correct for small differences in loading. The resulting bands on film were quantitated by computer-assisted video densitometry. Using the ImageJ 1.29x software (National Institutes of Health, Bethesda, MD), the protein band density was measured. The amount of protein under control conditions was assigned a relative value of 100%.

**VEGF enzyme-linked immunosorbent assay.** Cell culture media supernatants were frozen at −20°C until assayed for VEGF using a commercial enzyme-linked immunosorbent assay (ELISA) kit (R&D Systems). The supernatants were dispensed onto a microtiter plate coated with an anti-VEGF antibody that recognizes mouse $VEGF_{120, 164}$ and then sandwiched with a secondary anti-VEGF antibody conjugated to HRP. The resulting chromogenic reaction was stopped and read at 450 nm, and the concentration of VEGF was determined from the standard curve. VEGF concentrations were then corrected for the total protein concentrations and the data expressed as picogram VEGF per milligram protein.

**RT-PCR and sequencing.** Total RNA was purified with TRIzol (Invitrogen) from both dividing undifferentiated and differentiated podocytes. As a positive control, total RNA was also extracted from the cortex of a mouse kidney. The RNA was reverse transcribed to cDNA with avian myeloblastosis virus, random hexamers, and deoxynucleotides, as directed in the SuperScript kit (Invitrogen). The PCR primers for VEGFR-1 or -2 were added, along with deoxynucleotides and *Taq* polymerase (Invitrogen). For mouse VEGFR-1, the forward primer was 5′-CTC TGA TGG TGA TCG TGG-3′ and the reverse primer 5′-CAT GCC TCT GGC CAC TTG-3′ (34). For mouse VEGFR-2, the forward primer was 5′-GCC AAT GAA GGG GAA CTG AAG AC-3′ and the reverse primer 5′-TCT GGC TGC TGG TGA TGC TGT C-3′ (modified from the rat sequence) (35). PCR was performed under the following conditions: denaturation at 94°C for 2 min, 40 cycles of denaturation at 94°C for 1 min, annealing at 58°C for VEGFR-1 and 53°C for VEGFR-2 for 30 s, and extension at 72°C for 1 min, followed by final extension at 72°C for 4 min. An aliquot of the final PCR product was run in a 2% agarose gel stained with ethidium bromide. The predicted band sizes were 317 bp for VEGFR-1 and 538 bp for VEGFR-2. The remainder of the PCR product was cleaned up with a PCR purification kit (QIAquick; Qiagen, Valencia, CA) and sequenced in both directions with the forward and reverse primers (University of Pennsylvania DNA Sequencing Facility). The elucidated sequence of the RT-PCR product was compared with the published mRNA sequence with the aid of a sequence analysis program (MacVector; Accelrys, San Diego, CA).

**Immunofluorescent staining.** Podocytes were seeded onto collagen I–coated four-chamber slides (Nunclon, Roskilde, Denmark) and allowed to differentiate over 2 weeks at 37.5°C. Chambers were washed three times in 1× PBS for 5 min. Cells were then fixed in a 50:50 mixture of methanol:acetone for 8 min at −20°C. Afterward, 0.1% triton X-100 in PBS was added for 3 min to permeabilize the cells. Nonspecific binding sites were blocked with 1% BSA in PBS for 1 h at room temperature. The four chambers were treated with the following primary antibodies at a 1:500 dilution in 1% BSA: *1*) anti–VEGFR-1 antibody alone, *2*) anti–VEGFR-1 antibody preabsorbed overnight with 10 times the volume of VEGFR-1 blocking peptide, *3*) anti–VEGFR-1 antibody preabsorbed with 10 times the volume of clusterin (irrelevant blocking peptide), and *4*) no primary antibody. This setup was duplicated for the anti–VEGFR-2 antibody. After a 2-h incubation at room temperature, the chambers were washed three times in 1× PBS, and a Cy3-conjugated donkey anti-rabbit antibody (Jackson ImmunoResearch) was added at a 1:1,000 dilution in 1% BSA. The secondary antibody was allowed to incubate in the dark for 1 h at room temperature. After three more 5-min washes in 1× PBS and one brief wash in $dH_2O$, a 1:10,000 dilution of 4′,6-diamidino-2-phenylindole (DAPI) (Molecular Probes, Eugene, OR) was added to each chamber for 30 s to stain nuclei. The plastic chambers were then removed and the slide mounted under a coverslip in fluorescence mounting medium (Kirkegaard & Perry Laboratories, Gaithersburg, MD). Photomicrographs of each section of the slides were taken at 200× magnification with a fluorescence microscope (Nikon Eclipse E600) connected to a charge-coupled device digital camera (CoolSNAP cf.; Roper Scientific, Trenton, NJ). Fluorescence was imaged separately for standardized times in the red and blue channels for Cy3 and DAPI. A brightfield image was obtained using differential interference contrast (or Nomarski) microscopy. Finally, the fluorescent and brightfield images were electronically merged using the IPLab Mac software (Scanalytics, Fairfax, VA).

**Statistical analysis.** Graphical data are displayed as means ± SE for the number of independent experiments indicated in the figure legends. Unpaired Student's *t* test was used to compare the control with the experimental group. $P < 0.05$ was considered statistically significant.

## RESULTS

**Exogenous VEGF stimulated α3(IV) but did not affect α5(IV) collagen production in podocytes.** Cultured podocytes were exposed to exogenous mouse in doses of 2, 8, and 20 ng/ml VEGF$_{164}$. By Western blot analysis, all of the VEGF doses significantly stimulated the production of α3(IV) protein by 52–73% at 24 h (Fig. 1*A*). When exogenous VEGF stimulation was continued for 48 h, α3(IV) collagen production reached a peak (80% increase) at 8 ng/ml VEGF then tapered off at 20 ng/ml (Fig. 1*A*). The control level of α3(IV) collagen at 48 h was greater than at 24 h, suggesting the ongoing production of collagen over time. The degree of VEGF-stimulated α3(IV) production was not affected by SB-431542, a TGF-β signaling inhibitor (33) (*n* = 6, *P* = NS for VEGF vs. VEGF plus SB-431542).

Similarly designed studies were conducted to assay the effect of VEGF on the production of α5(IV) collagen measured by immunoblotting. At the VEGF doses and treatment times used, VEGF had no significant effect on the production of α5(IV) collagen (Fig. 1*B*).

**Blockade of VEGF signaling decreased basal and VEGF-stimulated levels of α3(IV) collagen.** The VEGF receptor tyrosine kinase proteins are specifically blocked by SU5416 at an IC$_{50}$ of ~1 μmol/l for the inhibition of VEGFR-1 and -2 autophosphorylation (15,32). SU5416 dose-dependently diminished the production of α3(IV) collagen in the basal state, reaching a plateau at ~5 μmol/l SU5416 (Fig. 2*A*). Downstream of the receptors, VEGF can signal through the PI3K-Akt pathway, so the PI3K inhibitor, LY294002, was also tested; this treatment progressively decreased the basal production of α3(IV) protein (Fig. 2*B*), similar to SU5416 (Fig. 2*A*). When 8 ng/ml exogenous VEGF was added for 48 h, the increase in α3(IV) protein was completely prevented by the concurrent addition of 1 μmol/l SU5416 (Fig. 2*C*). This intermediate dose of SU5416 did not reduce the basal amount of α3(IV) collagen. However, a higher dose of SU5416 (5 μmol/l) not only prevented exogenous VEGF from stimulating α3(IV) production but also depressed the basal α3(IV) collagen level (Fig. 2*C*), consistent with the notion that SU5416 can inhibit the effect of endogenously produced VEGF.

**VEGFR-1, but not -2, was detectable in podocytes by RT-PCR.** The RT-PCR product for VEGFR-1 was detected at the appropriate size in differentiated mouse podocytes, but none were detected for VEGFR-2 (Fig. 3*A*). Failure to identify VEGFR-2 was not due to technical problems because the correct-sized band for VEGFR-2 was readily amplified from mouse kidney cortex (Fig. 3*A*). In addition, RT-PCR did not identify VEGFR-2 mRNA in dividing undifferentiated podocytes (data not shown). To prove that the VEGFR-1 band had originated from mRNA and not from contaminating genomic DNA, the addition of RNase before the RT-PCR procedure completely abrogated the band (data not shown). Finally, the VEGFR-1 band was sequenced and found to align perfectly with the published mRNA sequence for mouse VEGFR-1 (gi:34328179) (Fig. 3*B*).

**Detection of VEGFR-1 protein.** The Western blot analysis for VEGFR-1 showed a band at ~180 kDa (Fig. 4*A*). However, preincubation of the anti–VEGFR-1 antibody with increasing doses of a specific blocking peptide before immunoblotting progressively competed away the intensity of the band (Fig. 4*A*). Moreover, the addition of an irrelevant blocking peptide, clusterin, did not dampen the intensity of the band (Fig. 4*A*), proving the specificity of the antibody for VEGFR-1.

In contrast, the Western blot analysis for VEGFR-2 showed a band that was not at the expected size of 180 kDa but at 110 kDa (Fig. 4*B*), which was likely the result of nonspecific binding of the anti–VEGFR-2 antibody since the band did not fade with increasing doses of the blocking peptide (Fig. 4*B*). Thus, VEGFR-2 protein is probably absent from cultured mouse podocytes, which is consistent with the RT-PCR data (Fig. 3*A*).

**Visualization and functioning of the VEGFR-1 protein.** Corroborative immunostaining for the VEGF receptor proteins was performed in the podocyte. The stain for VEGFR-1 protein showed a strong fluorescent signal (red color) localized to the cell body of the podocyte (Fig. 5*A*). Furthermore, preincubation of the anti–VEGFR-1 antibody with a blocking peptide largely abrogated the immunostaining (Fig. 5*B*), decreasing the fluorescent signal down to background levels seen with the negative control, in which the primary antibody was omitted (Fig. 5*D*). Finally, the addition of an irrelevant blocking peptide, clusterin, to the anti–VEGFR-1 antibody did not compete away the intensity of the immunofluorescence (Fig. 5*C*). In contrast, the immunostaining for VEGFR-2 was almost nil under all the specificity conditions tested as above (Fig. 5*E–H*).

Autophosphorylation of VEGFR-1 was sought as evidence for the initiation of VEGF signaling in podocytes. After stimulation with recombinant mouse VEGF$_{164}$ for 0.5 h, the amount of phospho–VEGFR-1 was detectable above background (Fig. 6). With continued VEGF stimulation, VEGFR-1 became increasingly phosphorylated, reaching a peak at ~18 h (Fig. 6). Elevated phospho–VEGFR-1 levels were sustained for the remainder of the experiment. On the other hand, total VEGFR-1 and β-actin levels stayed relatively constant (Fig. 6).

**Endogenous VEGF partly mediated TGF-β1 stimulation of α3(IV) collagen but not TGF-β1 inhibition of α5(IV) collagen.** Consistent with our previous data (21), addition of 2 ng/ml TGF-β1 for 48 h increased the production of endogenous VEGF by 2.7-fold; the media supernatant level of mouse VEGF$_{120, 164}$, measured by ELISA (R&D Systems), increased from 111 ± 8.5 pg VEGF/mg protein to 294 ± 31.4 pg VEGF/mg protein (*n* = 5, *P* < 0.001 vs. control). Concomitantly, 2 ng/ml TGF-β1 stimulated α3(IV) protein production by 2.3-fold (Fig. 7*A*), a response that was completely prevented by pretreatment with 1 μmol/l SB-431542, a direct inhibitor of TGF-β signaling (33). On the other hand, stimulation of α3(IV) collagen production by TGF-β1 was partially and significantly prevented by pretreatment with either 5 μmol/l SU5416 (VEGF receptor inhibitor) or 25 μmol/l LY294002 (PI3K inhibitor). Additionally, Fig. 7*A* shows that α3(IV) collagen levels under control conditions were decreased by treatment with SU5416 or LY294002, further suggesting that endogenous VEGF maintains a small component of the basal α3(IV) production in podocytes (Fig. 2*A–C*).

In contrast, 2 ng/ml TGF-β1 decreased α5(IV) collagen levels in mouse podocytes (Fig. 7*B*) as previously described (21). TGF-β1–mediated suppression of α5(IV) col-
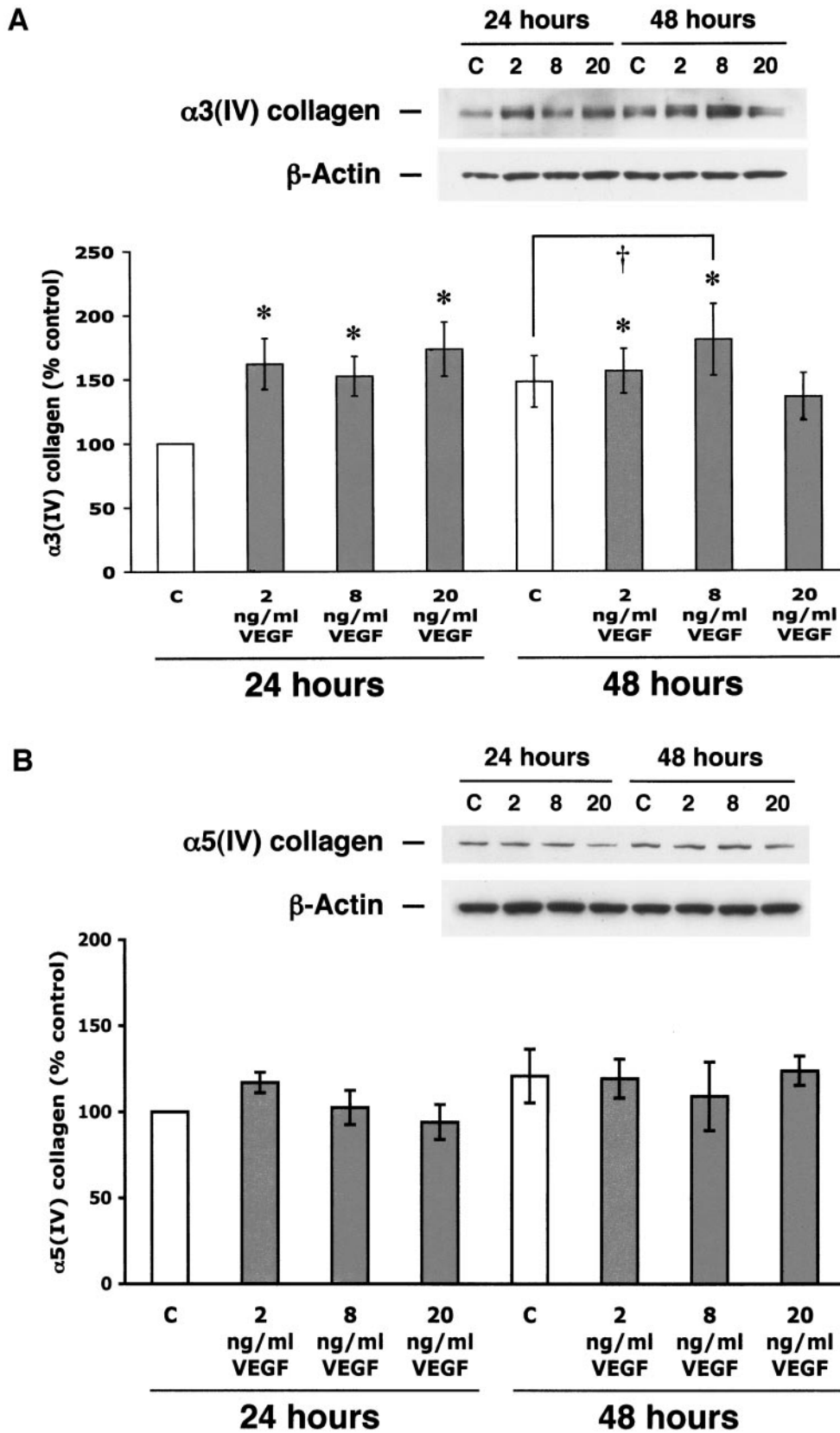
FIG. 1. Cultured, differentiated mouse podocytes were treated with 2, 8, or 20 ng/ml recombinant mouse $VEGF_{164}$ for 24 or 48 h. *A*: Compared with the control (C) at 24 h, VEGF at all three doses significantly increased production of the α3(IV) collagen chain by ~52–80%, with the maximal effect seen at 8 ng/ml VEGF for 48 h ($n = 10$). *$P < 0.05$ vs. 24-h control; †$P < 0.05$ vs. 48-h control. *B*: VEGF did not significantly affect production of the α5(IV) collagen chain ($n = 5$).
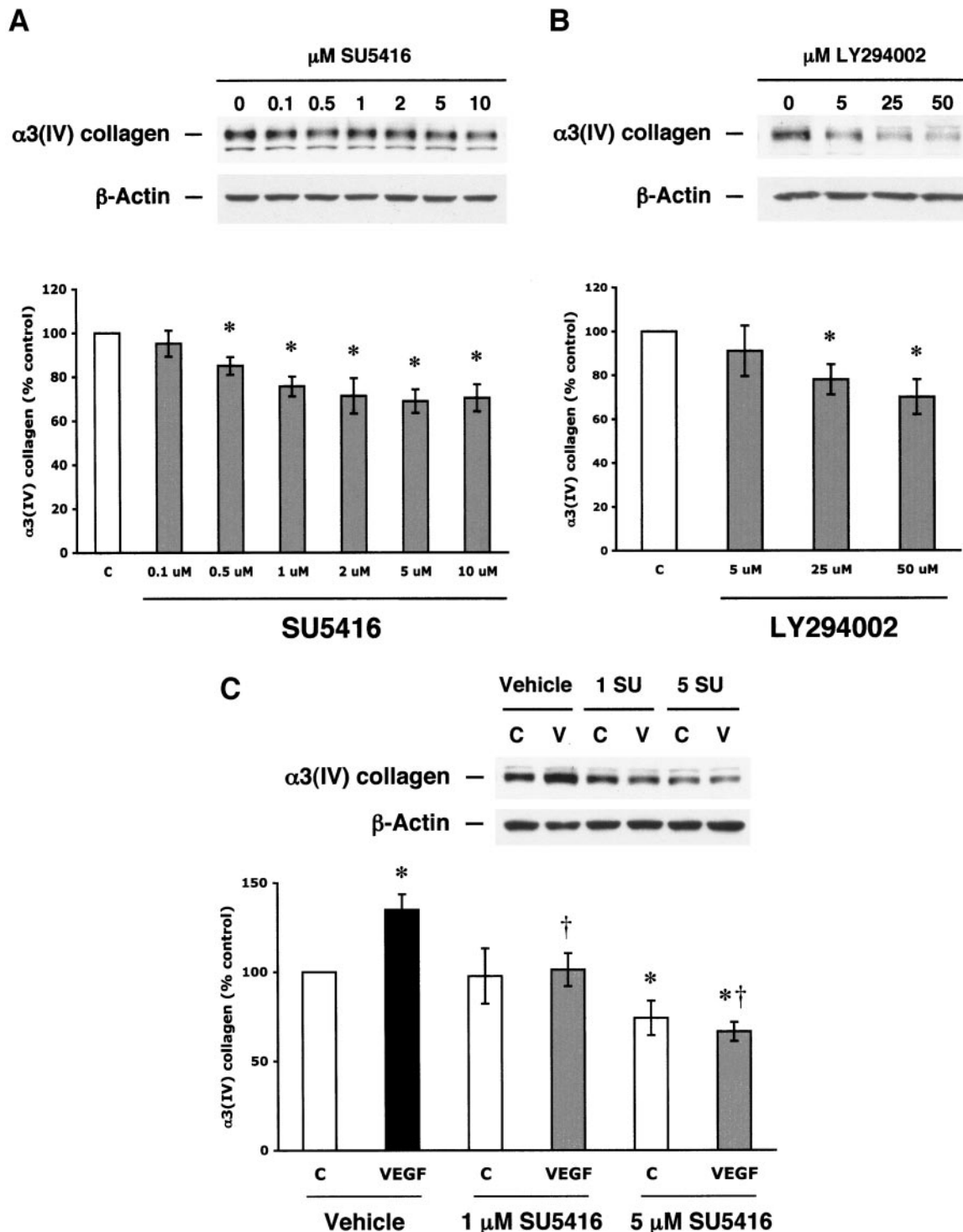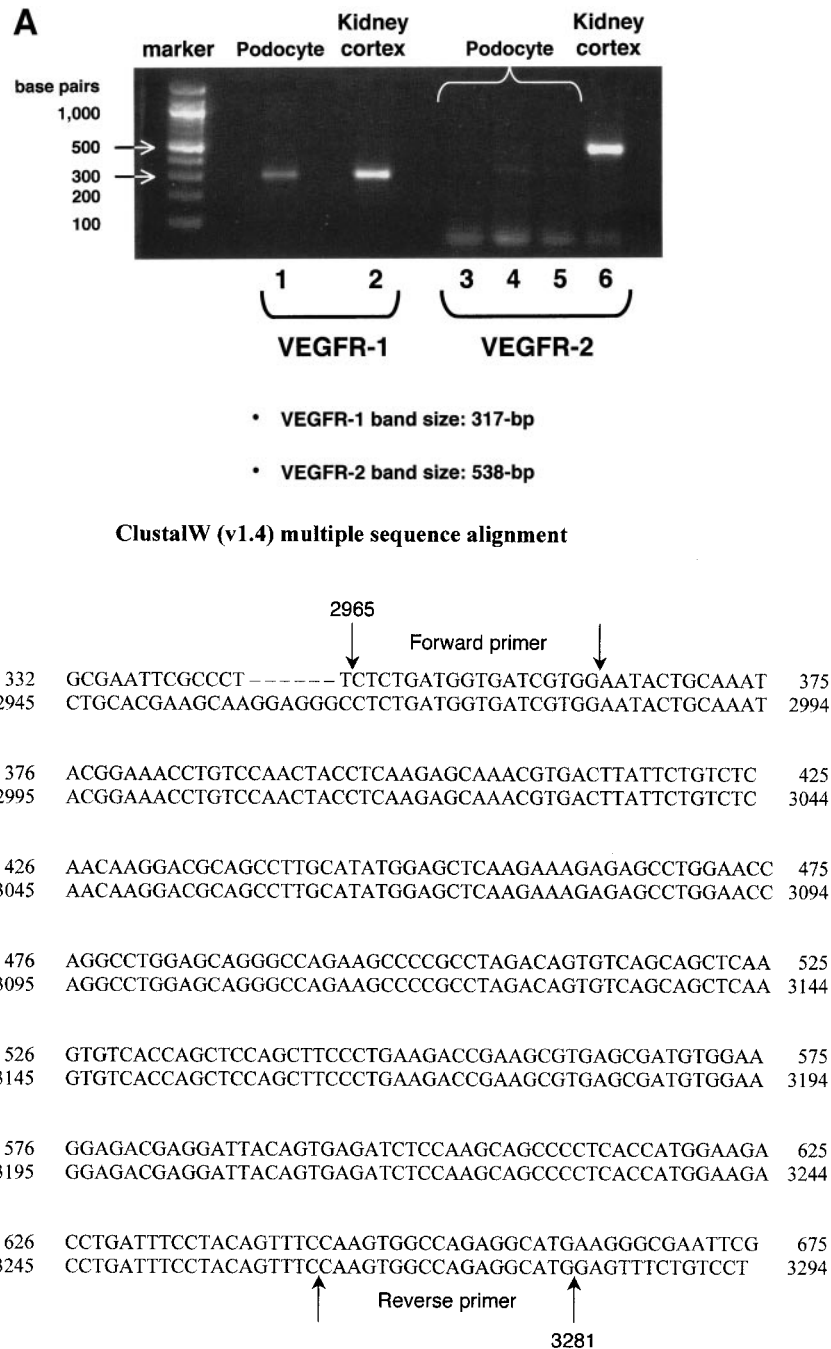
FIG. 2. *A*: Increasing doses of the VEGF receptor inhibitor, SU5416, for 48 h gradually suppressed the basal podocyte production of $\alpha3(IV)$ collagen, as seen by Western blot analysis ($n = 5$). *B*: The PI3K inhibitor, LY294002, dose-dependently decreased basal $\alpha3(IV)$ collagen production over the course of 48 h ($n = 7$). *C*: At 8 ng/ml for 48 h, VEGF-stimulated $\alpha3(IV)$ collagen production was completely abolished by concurrent treatment with 1 $\mu$mol/l SU5416 (SU) and further suppressed by 5 $\mu$mol/l SU5416, suggesting that endogenous VEGF (V) is needed to maintain $\alpha3(IV)$ collagen production in the podocyte ($n = 7$). *A–C*: *$P < 0.05$ vs. control; †$P < 0.05$ vs. VEGF. C, control.

lagen was not significantly changed by SU5416 treatment (Fig. 7*B*), which is consistent with the data that VEGF had no effect on the production of $\alpha5(IV)$ collagen (Fig. 1*B*). However, the inhibitory effect of TGF-$\beta$1 on $\alpha5(IV)$ production could be successfully reversed by the TGF-$\beta$ signaling inhibitor, SB-431542 (Fig. 7*B*), indicating that the

effect of TGF-$\beta$1 on $\alpha5(IV)$ is dependent upon the TGF-$\beta$ receptor system but not the VEGF receptor system.

To exclude the possibility that either SU5416 or LY294002 was interfering directly with the TGF-$\beta$1 signaling system, we assessed the effects of these inhibitors on the phosphorylation of Smad2, a major intracellular sig-

**A**



- VEGFR-1 band size: 317-bp

- VEGFR-2 band size: 538-bp

**B**

**ClustalW (v1.4) multiple sequence alignment**



FIG. 3. *A*: RT-PCR revealed message for VEGFR-1 (*lane 1*, 317 bp) but not VEGFR-2 (*lanes 3–5*, 538 bp) in differentiated mouse podocytes. Mouse kidney cortex served as the positive control (*lanes 2* and *6*). *B*: The nucleotide sequence of the RT-PCR product for VEGFR-1 matched perfectly with the published sequence of mouse VEGFR-1 mRNA (gi:34328179).

naling protein downstream of the TGF-β receptor system (36). Smad2 was examined because a commercial antibody against phospho-Smad2 is available. The parallel arm of TGF-β1 signaling, the Smad3 pathway, was not investigated because an antibody against phospho-Smad3 has not been made available. Treatment with exogenous TGF-β1 markedly increased phospho-Smad2 levels in the podocyte (Fig. 7C). As expected, Smad2 phosphorylation was totally suppressed by the direct TGF-β inhibitor, SB-431542 (Fig. 7C). However, Smad2 phosphorylation was not inhibited by either SU5416 or LY294002 (Fig. 7C).

## DISCUSSION

VEGF comprises a family of potent cytokines that include the VEGF-A class and the less well-described VEGF-B, -C, -D, and -E classes. In the VEGF-A class, differential exon splicing gives rise to at least five different VEGF isoforms (37–39) that have been named according to the number of amino acids they contain. In humans, they are designated $VEGF_{121}$, $VEGF_{145}$, $VEGF_{165}$, $VEGF_{189}$, and $VEGF_{206}$; in mice, the VEGF isoforms have one less amino acid and are called $VEGF_{120}$, $VEGF_{164}$, $VEGF_{188}$, and $VEGF_{205}$ (40). In general, the smaller isoforms ($VEGF_{120, 164}$) are solu-
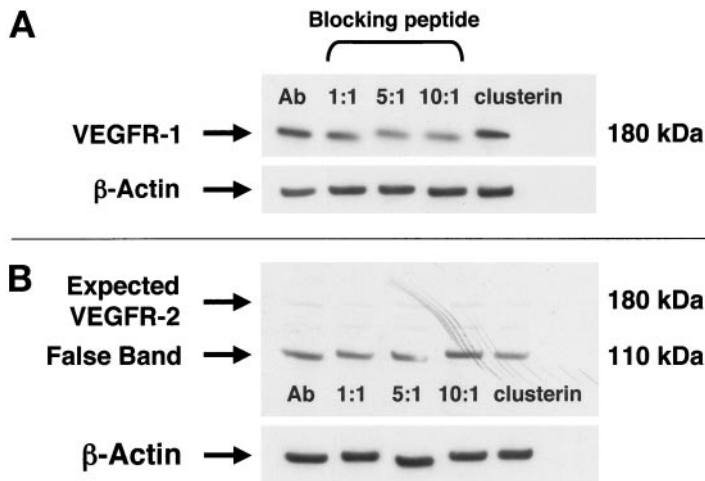
**FIG. 4.** *A*: **The Western blot analysis band for VEGFR-1 protein in podocytes (~180 kDa) was gradually reduced in intensity by increasing ratios of blocking peptide to anti–VEGFR-1 antibody but not by an irrelevant blocking peptide (clusterin), thus proving the antibody's specificity.** *B*: **The Western blot analysis band for the VEGFR-2 protein appeared at an unexpected size (110 kDa), and its density was not reduced by increasing doses of VEGFR-2–blocking peptide.**

ble and freely secreted, whereas the larger isoforms (VEGF$_{188, 205}$) remain cell associated (41). Nevertheless, the predominant species is VEGF$_{165}$, the most abundantly expressed and secreted isoform (13). The major source of VEGF in the glomerulus is the podocyte (9), and this cell can be stimulated to overproduce VEGF by cytokines such as TGF-$\beta$1 (21) and by pathophysiological states such as diabetes (5). The functions of podocyte-derived VEGF are not well established, but recent studies have implicated an important role in the pathogenesis of albuminuria in type 1 and type 2 diabetes (7,8). It remains unclear, though, how VEGF can influence macromolecular permeability across the glomerular filtration barrier or even what cell type VEGF acts upon.

Several lines of evidence support the existence of a functional VEGF autocrine loop in cultured podocytes. First, exogenous VEGF$_{164}$ exerts a measurable effect on podocyte pathobiology in the form of increased $\alpha$3(IV) collagen production, a meaningful parameter given the podocyte's role in GBM assembly. That the enhanced production of $\alpha$3(IV) collagen was completely blocked by SU5416 attests to the involvement of the VEGF signaling system in mediating $\alpha$3(IV) collagen expression. Not only did SU5416 completely prevent VEGF-induced $\alpha$3(IV) collagen, but increasing doses of SU5416 gradually decreased $\alpha$3(IV) below control levels, indicating a functional role for endogenous VEGF in basal $\alpha$3(IV) production. The range of SU5416 doses was chosen to encompass the IC$_{50}$ of ~1 $\mu$mol/l for the inhibition of VEGFR-1 and -2 autophosphorylation but not to infringe on the IC$_{50}$ of ~20 $\mu$mol/l for the
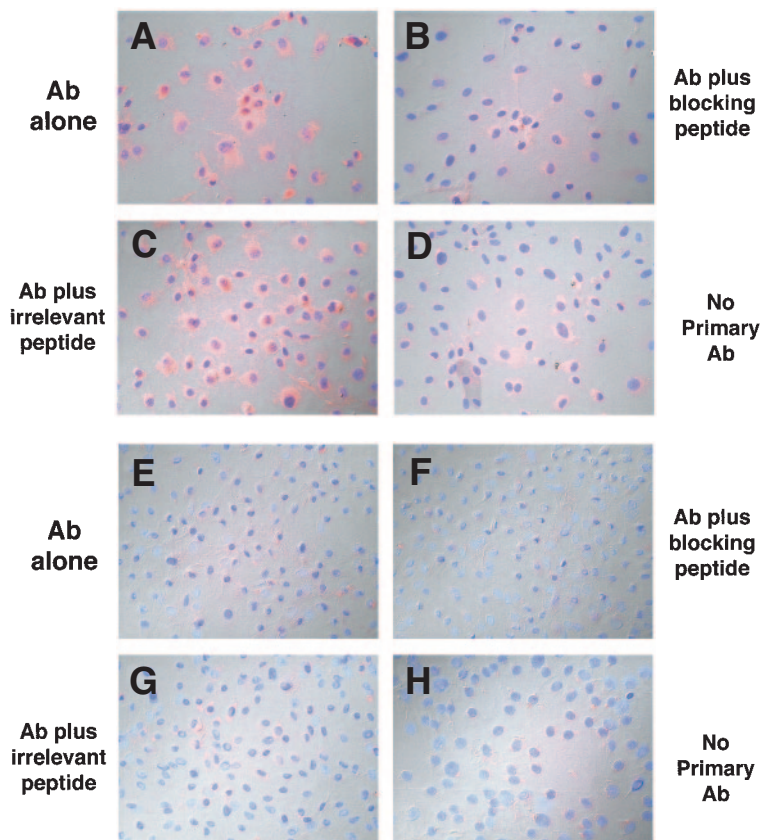


**FIG. 5. Immunofluorescent staining of cultured mouse podocytes demonstrated VEGFR-1 protein, visible as a red fluorescence signal (*A*), that was largely abrogated by the addition of VEGFR-1–blocking peptide to the anti–VEGFR-1 primary antibody (Ab) (*B*). However, the irrelevant blocking peptide (clusterin) did not affect the intensity of the red signal (*C*). Omission of the primary antibody, a negative control, showed minimal background fluorescence (*D*). The setup of immunostaining for VEGFR-2 was identical to that for VEGFR-1. VEGFR-2 protein was not detected under any of the specificity conditions (*E–H*). DAPI was used to stain the nuclei blue.**
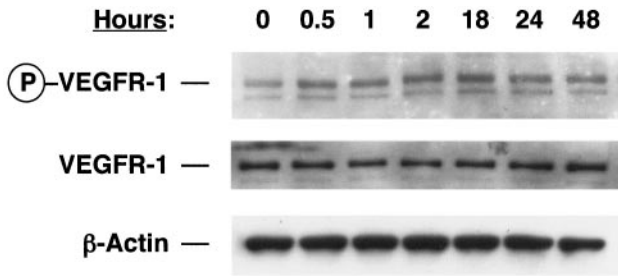
**FIG. 6: Treatment of podocytes with 8 ng/ml VEGF for the indicated times (0–48 h) resulted in increasing levels of tyrosine-autophosphorylated VEGFR-1, already evident at 0.5 h and sustained for 48 h. The pool of total VEGFR-1 and β-actin remained relatively unchanged.**

inhibition of platelet-derived growth factor–dependent phosphorylation (15,32).

That VEGF exerts a substantive effect on podocytes is reinforced by the identification of VEGFR-1, the demonstration of receptor autophosphorylation, and the inhibition of exogenous and endogenous VEGF effects by the receptor inhibitor, SU5416, and by the PI3K inhibitor, LY294002. The presence of VEGFR-1 mRNA and protein was confirmed by RT-PCR, immunoblotting, and fluorescence immunocytochemistry in mouse podocytes. In contrast, VEGFR-2 was undetectable by these means. Our findings extend those of Foster et al. (10) who detected a message for VEGFR-1, but not -2, by RT-PCR in human podocytes. Since treatment with VEGF results in tyrosine phosphorylation of VEGFR-1, signaling through this receptor is potentially responsible for the effects of VEGF on collagen production. It is less likely that the other VEGF receptors known to be present in podocytes (10) can
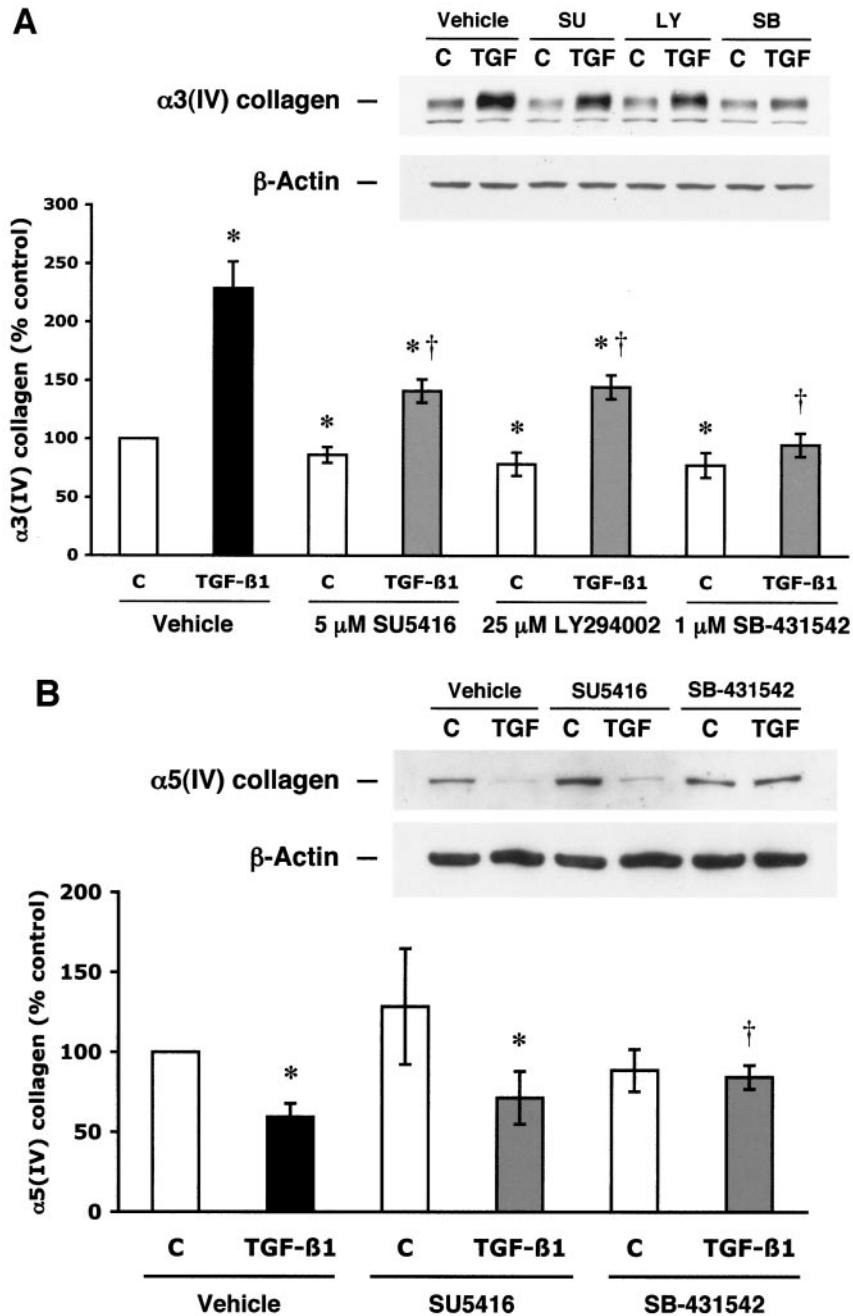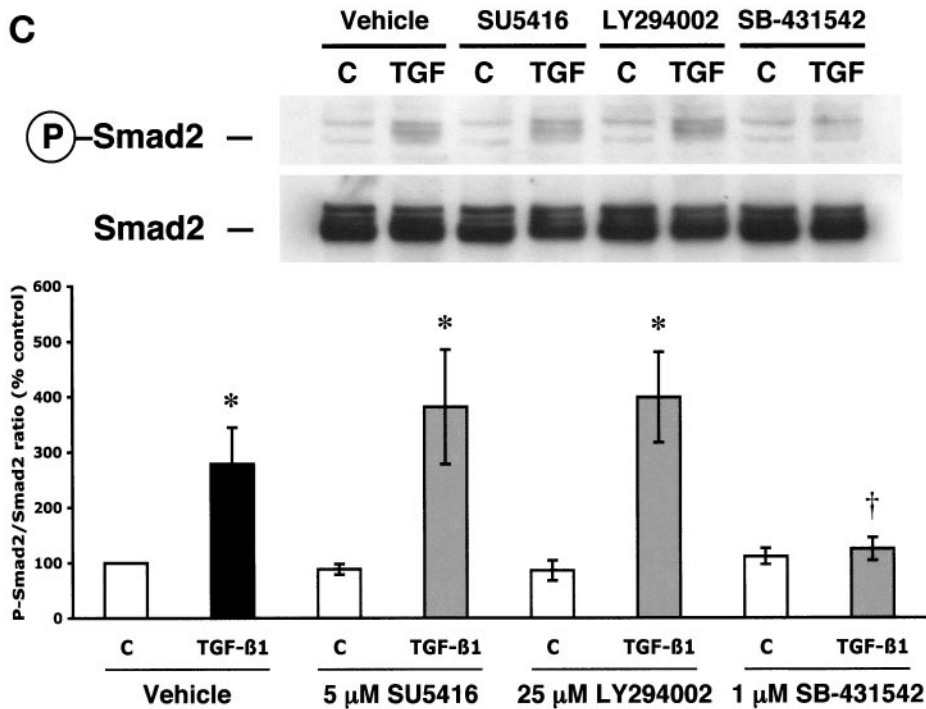
FIG. 7. *A*: At 2 ng/ml for 48 h, TGF-β1–stimulated production of α3(IV) collagen was reduced by almost 70% with either 5 μmol/l SU5416 (SU), a VEGF receptor inhibitor, or 25 μmol/l LY294002 (LY), a PI3K inhibitor, but was completely prevented by 1 μmol/l SB-431542 (SB), a TGF-β signaling inhibitor. In addition, basal levels of α3(IV) collagen were significantly decreased by all three inhibitors (*n* = 6). *B*: At 2 ng/ml for 48 h, the TGF-β1–suppressed production of α5(IV) collagen was not significantly affected by 5 μmol/l SU5416 but was reversed by 1 μmol/l SB-431542 (*n* = 5). *C*: Neither 5 μmol/l SU5416 nor 25 μmol/l LY294002 inhibited Smad2 phosphorylation by TGF-β1. However, TGF-β1–induced phospho-Smad2 was completely blocked by 1 μmol/l SB-431542 (*n* = 5). *A–C*: *P* < 0.05 vs. control; †*P* < 0.05 vs. TGF-β1. C, control.

transduce the stimulatory effect of VEGF on α3(IV) collagen production; VEGFR-3 responds only to VEGF-C or -D (42), and neuropilin-1 does not signal by itself (43) but acts more like a coreceptor for VEGFR-2 (14).

Additional proof for the existence of a VEGF autocrine loop in podocytes was obtained by stimulating endogenous VEGF secretion by TGF-β1 (21) and then being able to inhibit an effect of TGF-β1 with anti-VEGF therapy. Both SU5416 and LY294002 reduced the TGF-β1–induced α3(IV) collagen by nearly 70%, suggesting that part of the mechanism for TGF-β1 to increase α3(IV) collagen is mediated by the VEGF system, signaling through the PI3K-Akt pathway. This partial inhibition also implies that TGF-β1 stimulates a component of α3(IV) production that is not mediated by endogenous VEGF or PI3K-Akt signaling. However, the entire TGF-β1 effect on α3(IV) collagen could be inhibited by SB-431542, which blocks all avenues of TGF-β1 signaling by inhibiting the TGF-β type I receptor kinase (21,33). It should be noted that neither SU5416 nor LY294002 directly inhibited the TGF-β1 signaling pathway, evidenced by lack of effect on Smad2 phosphorylation. On the other hand, treatment with SB-431542 completely abolished Smad2 phosphorylation following TGF-β1 treatment. We conclude that the autocrine VEGF system in cultured podocytes mediates part of the TGF-β1 stimulatory effect on α3(IV) collagen production, possibly through VEGFR-1 and the PI3K pathway.

To further establish the specificity of SU5416 in podocytes, we investigated a cytokine-mediated end point that does not involve the VEGF pathway. TGF-β1 strongly inhibits α5(IV) collagen production (21), whereas VEGF neither increases nor decreases α5(IV) production (Fig. 1*B*). Therefore, TGF-β1 does not utilize the endogenous VEGF system to suppress α5(IV) collagen. Accordingly, SU5416 fails to modify the inhibitory effect of TGF-β1 on α5(IV) production (Fig. 7*B*). TGF-β1–mediated suppression of α5(IV) collagen, however, can be reversed by a direct inhibitor of TGF-β signaling, SB-431542 (Fig. 7*B*). Combined with the prior results on α3(IV) collagen, the fact that SU5416 can inhibit a VEGF-dependent effect of TGF-β1 (e.g., on α3) but not a VEGF-independent effect of TGF-β1 (e.g., on α5) demonstrates that SU5416 specifically targets the VEGF pathway.

The novel role of VEGF in mediating some matrix-promoting effects of TGF-β1 in podocytes is distinct from its classically described properties relating to angiogenesis and vascular permeability and can be added to the expanding repertoire of VEGF actions in normal and pathophysiologic states (44). For diabetic glomerulopathy, a revised pathogenetic scheme can be conceived that incorporates this newly discovered role for an autocrine VEGF loop in promoting podocyte expression of α3(IV) collagen, a principal ingredient of the GBM. The diabetic state gives rise to increased glomerular concentrations of TGF-β1 (45,46), whether coming from the mesangial cell in response to high glucose (47) or locally increased levels of angiotensin II (48) or from the glomerular endothelium in response to amadori-glycated albumin (49) or leptin (50). Increased levels of TGF-β1 can act in a paracrine manner upon the podocyte, now poised to respond to TGF-β1 because of concordant upregulation of the signaling TGF-β type II receptor (21). In this article, we show that one important consequence of TGF-β system overactivity in diabetic glomerulopathy is to stimulate podocyte secretion of VEGF and the actions thereof, such as increasing α3(IV) collagen production. This effect of TGF-β1 may be amplified by high ambient glucose, which increases both VEGF expression and α3(IV) collagen production in podocytes (21).

Whether stimulation of α3(IV) production by the TGF-β1–VEGF axis contributes to diabetic GBM thickening will need to be evaluated in animal models. In addition, the lack of a role for VEGF in modulating the inhibitory effect of TGF-β1 on α5(IV) collagen may have important conse-

quences. Excess α3(IV) collagen and decreased α5(IV) collagen production may disrupt the orderly assembly of the GBM framework, causing dysfunction of the glomerular filtration barrier. Perhaps VEGF-mediated dysregulation of GBM composition may help to explain why anti-VEGF therapy ameliorates albuminuria in diabetic nephropathy (7,8).

## ACKNOWLEDGMENTS

## REFERENCES

1. Leung DW, Cachianes G, Kuang WJ, Goeddel DV, Ferrara N: Vascular endothelial growth factor is a secreted angiogenic mitogen. *Science* 246:1306–1309, 1989
2. Dvorak HF, Brown LF, Detmar M, Dvorak AM: Vascular permeability factor/vascular endothelial growth factor, microvascular hyperpermeability, and angiogenesis. *Am J Pathol* 146:1029–1039, 1995
3. Senger DR, Galli SJ, Dvorak AM, Perruzzi CA, Harvey VS, Dvorak HF: Tumor cells secrete a vascular permeability factor that promotes accumulation of ascites fluid. *Science* 219:983–985, 1983
4. Cui TG, Foster RR, Saleem MA, Mathieson PW, Gillatt DA, Bates DO, Harper SJ: Differentiated human podocytes endogenously express an inhibitory isoform of vascular endothelial growth factor (VEGF$_{165}$b) mRNA and protein. *Am J Physiol Renal Physiol* 286:F767–F773, 2004
5. Cooper ME, Vranes D, Youssef S, Stacker SA, Cox AJ, Rizkalla B, Casley DJ, Bach LA, Kelly DJ, Gilbert RE: Increased renal expression of vascular endothelial growth factor (VEGF) and its receptor VEGFR-2 in experimental diabetes. *Diabetes* 48:2229–2239, 1999
6. Senthil D, Choudhury GG, McLaurin C, Kasinath BS: Vascular endothelial growth factor induces protein synthesis in renal epithelial cells: a potential role in diabetic nephropathy. *Kidney Int* 64:468–479, 2003
7. De Vriese AS, Tilton RG, Elger M, Stephan CC, Kriz W, Lameire NH: Antibodies against vascular endothelial growth factor improve early renal dysfunction in experimental diabetes. *J Am Soc Nephrol* 12:993–1000, 2001
8. Flyvbjerg A, Dagnaes-Hansen F, De Vriese AS, Schrijvers BF, Tilton RG, Rasch R: Amelioration of long-term renal changes in obese type 2 diabetic mice by a neutralizing vascular endothelial growth factor antibody. *Diabetes* 51:3090–3094, 2002
9. Simon M, Gröne HJ, Jöhren O, Kullmer J, Plate KH, Risau W, Fuchs E: Expression of vascular endothelial growth factor and its receptors in human renal ontogenesis and in adult kidney. *Am J Physiol* 268:F240–F250, 1995
10. Foster RR, Hole R, Anderson K, Satchell SC, Coward RJ, Mathieson PW, Gillatt DA, Saleem MA, Bates DO, Harper SJ: Functional evidence that vascular endothelial growth factor may act as an autocrine factor on human podocytes. *Am J Physiol Renal Physiol* 284:F1263–F1273, 2003
11. Eremina V, Sood M, Haigh J, Nagy A, Lajoie G, Ferrara N, Gerber HP, Kikkawa Y, Miner JH, Quaggin SE: Glomerular-specific alterations of VEGF-A expression lead to distinct congenital and acquired renal diseases. *J Clin Invest* 111:707–716, 2003
12. Ziyadeh FN, Wolf G: Why should an angiogenic factor modulate tubular structure in diabetic nephropathy? Some answers, more questions. *Kidney Int* 64:758–759, 2003
13. Ferrara N, Gerber HP, LeCouter J: The biology of VEGF and its receptors. *Nat Med* 9:669–676, 2003
14. Soker S, Takashima S, Miao HQ, Neufeld G, Klagsbrun M: Neuropilin-1 is expressed by endothelial and tumor cells as an isoform-specific receptor for vascular endothelial growth factor. *Cell* 92:735–745, 1998
15. Mendel DB, Laird AD, Smolich BD, Blake RA, Liang C, Hannah AL, Shaheen RM, Ellis LM, Weitman S, Shawver LK, Cherrington JM: Development of SU5416, a selective small molecule inhibitor of VEGF receptor tyrosine kinase activity, as an anti-angiogenesis agent. *Anticancer Drug Des* 15:29–41, 2000
16. Manley PW, Martiny-Baron G, Schlaeppi JM, Wood JM: Therapies directed at vascular endothelial growth factor. *Expert Opin Investig Drugs* 11:1715–1736, 2002
17. Huang K, Andersson C, Roomans GM, Ito N, Claesson-Welsh L: Signaling properties of VEGF receptor-1 and -2 homo- and heterodimers. *Int J Biochem Cell Biol* 33:315–324, 2001
18. Jiang BH, Zheng JZ, Aoki M, Vogt PK: Phosphatidylinositol 3-kinase signaling mediates angiogenesis and expression of vascular endothelial growth factor in endothelial cells. *Proc Natl Acad Sci U S A* 97:1749–1753, 2000
19. Qi JH, Matsumoto T, Huang K, Olausson K, Christofferson R, Claesson-Welsh L: Phosphoinositide 3 kinase is critical for survival, mitogenesis and migration but not for differentiation of endothelial cells. *Angiogenesis* 3:371–380, 1999
20. Lal BK, Varma S, Pappas PJ, Hobson RW 2nd, Duran WN: VEGF increases permeability of the endothelial cell monolayer by activation of PKB/akt, endothelial nitric-oxide synthase, and MAP kinase pathways. *Microvasc Res* 62:252–262, 2001
21. Iglesias-de la Cruz MC, Ziyadeh FN, Isono M, Kouahou M, Han DC, Kalluri R, Mundel P, Chen S: Effects of high glucose and TGF-β1 on the expression of collagen IV and vascular endothelial growth factor in mouse podocytes. *Kidney Int* 62:901–913, 2002
22. Hoshi S, Nomoto K, Kuromitsu J, Tomari S, Nagata M: High glucose induced VEGF expression via PKC and ERK in glomerular podocytes. *Biochem Biophys Res Commun* 290:177–184, 2002
23. Gruden G, Thomas S, Burt D, Zhou W, Chusney G, Gnudi L, Viberti G: Interaction of angiotensin II and mechanical stretch on vascular endothelial growth factor production by human mesangial cells. *J Am Soc Nephrol* 10:730–737, 1999
24. Chen S, Jim B, Ziyadeh FN: Diabetic nephropathy and transforming growth factor-β: transforming our view of glomerulosclerosis and fibrosis build-up. *Semin Nephrol* 23:532–543, 2003
25. Caramori ML, Kim Y, Huang C, Fish AJ, Rich SS, Miller ME, Russell G, Mauer M: Cellular basis of diabetic nephropathy. 1. Study design and renal structural-functional relationships in patients with long-standing type 1 diabetes. *Diabetes* 51:506–513, 2002
26. White KE, Bilous RW: Type 2 diabetic patients with nephropathy show structural-functional relationships that are similar to type 1 disease. *J Am Soc Nephrol* 11:1667–1673, 2000
27. Myers BD, Nelson RG, Williams GW, Bennett PH, Hardy SA, Berg RL, Loon L, Knowler WC, Mitch WE: Glomerular function in Pima Indians with noninsulin dependent diabetes mellitus of recent onset. *J Clin Invest* 88:524–530, 1991
28. Makino H, Shikata K, Hayashi T, Wieslander J, Haramoto T, Hirata K, Wada J, Yoshida T, Yoshioka K, Ota Z: Immunoreactivity of the JK-132 monoclonal antibody directed against basement membrane collagen in normal and diabetic glomeruli. *Virchows Arch* 424:235–241, 1994
29. Funabiki K, Makita Y, Yamamoto M, Shike T, Fukui M, Sumiyoshi Y, Tomino Y: Dissociated expression of collagen type IV subchains in diabetic kidneys of KKAy mice. *Nephron* 80:208–213, 1998
30. Ledbetter S, Copeland EJ, Noonan D, Vogeli G, Hassell JR: Altered steady-state mRNA levels of basement membrane proteins in diabetic mouse kidneys and thromboxane synthase inhibition. *Diabetes* 39:196–203, 1990
31. Mundel P, Reiser J, Zúñiga-Mejía-Borja A, Pavenstädt H, Davidson G, Kriz W, Zeller R: Rearrangements of the cytoskeleton and cell contacts induce process formation during differentiation of conditionally immortalized mouse podocyte cell lines. *Exp Cell Res* 236:248–258, 1997
32. Fong TA, Shawver LK, Sun L, Tang C, App H, Powell TJ, Kim YH, Schreck R, Wang X, Risau W, Ullrich A, Hirth KP, McMahon G: SU5416 is a potent and selective inhibitor of the vascular endothelial growth factor receptor (Flk-1/KDR) that inhibits tyrosine kinase catalysis, tumor vascularization, and growth of multiple tumor types. *Cancer Res* 59:99–106, 1999
33. Callahan JF, Burgess JL, Fornwald JA, Gaster LM, Harling JD, Harrington FP, Heer J, Kwon C, Lehr R, Mathur A, Olson BA, Weinstock J, Laping NJ:

Identification of novel inhibitors of the transforming growth factor β1 (TGF-β1) type 1 receptor (ALK5). *J Med Chem* 45:999–1001, 2002

34. Mallet C, Feraud O, Ouengue-Mbele G, Gaillard I, Sappay N, Vittet D, Vilgrain I: Differential expression of VEGF receptors in adrenal atrophy induced by dexamethasone: a protective role of ACTH. *Am J Physiol Endocrinol Metab* 284:E156–E167, 2003

35. Inoue K, Sakurada Y, Murakami M, Shirota M, Shirota K: Detection of gene expression of vascular endothelial growth factor and flk-1 in the renal glomeruli of the normal rat kidney using the laser microdissection system. *Virchows Arch* 442:159–162, 2003

36. Massagué J, Wotton D: Transcriptional control by the TGF-β/Smad signaling system. *EMBO J* 19:1745–1754, 2000

37. Tischer E, Mitchell R, Hartman T, Silva M, Gospodarowicz D, Fiddes JC, Abraham JA: The human gene for vascular endothelial growth factor: multiple protein forms are encoded through alternative exon splicing. *J Biol Chem* 266:11947–11954, 1991

38. Houck KA, Ferrara N, Winer J, Cachianes G, Li B, Leung DW: The vascular endothelial growth factor family: identification of a fourth molecular species and characterization of alternative splicing of RNA. *Mol Endocrinol* 5:1806–1814, 1991

39. Poltorak Z, Cohen T, Sivan R, Kandelis Y, Spira G, Vlodavsky I, Keshet E, Neufeld G: VEGF145, a secreted vascular endothelial growth factor isoform that binds to extracellular matrix. *J Biol Chem* 272:7151–7158, 1997

40. Shima DT, Kuroki M, Deutsch U, Ng YS, Adamis AP, D'Amore PA: The mouse gene for vascular endothelial growth factor: genomic structure, definition of the transcriptional unit, and characterization of transcriptional and post-transcriptional regulatory sequences. *J Biol Chem* 271: 3877–3883, 1996

41. Park JE, Keller GA, Ferrara N: The vascular endothelial growth factor (VEGF) isoforms: differential deposition into the subepithelial extracellular matrix and bioactivity of extracellular matrix-bound VEGF. *Mol Biol Cell* 4:1317–1326, 1993

42. Karkkainen MJ, Makinen T, Alitalo K: Lymphatic endothelium: a new frontier of metastasis research. *Nat Cell Biol* 4:E2–E5, 2002

43. Neufeld G, Cohen T, Shraga N, Lange T, Kessler O, Herzog Y: The neuropilins: multifunctional semaphorin and VEGF receptors that modulate axon guidance and angiogenesis. *Trends Cardiovasc Med* 12:13–19, 2002

44. Kang DH, Johnson RJ: Vascular endothelial growth factor: a new player in the pathogenesis of renal fibrosis. *Curr Opin Nephrol Hypertens* 12:43–49, 2003

45. Ziyadeh FN, Hoffman BB, Han DC, Iglesias-de la Cruz MC, Hong SW, Isono M, Chen S, McGowan TA, Sharma K: Long-term prevention of renal insufficiency, excess matrix gene expression, and glomerular mesangial matrix expansion by treatment with monoclonal antitransforming growth factor-β antibody in *db/db* diabetic mice. *Proc Natl Acad Sci U S A* 97:8015–8020, 2000

46. Iwano M, Kubo A, Nishino T, Sato H, Nishioka H, Akai Y, Kurioka H, Fujii Y, Kanauchi M, Shiiki H, Dohi K: Quantification of glomerular TGF-β1 mRNA in patients with diabetes mellitus. *Kidney Int* 49:1120–1126, 1996

47. Ziyadeh FN, Sharma K, Ericksen M, Wolf G: Stimulation of collagen gene expression and protein synthesis in murine mesangial cells by high glucose is mediated by autocrine activation of transforming growth factor-β. *J Clin Invest* 93:536–542, 1994

48. Wolf G, Sharma K, Chen Y, Ericksen M, Ziyadeh FN: High glucose-induced proliferation in mesangial cells is reversed by autocrine TGF-β. *Kidney Int* 42:647–656, 1992

49. Chen S, Cohen MP, Lautenslager GT, Shearman CW, Ziyadeh FN: Glycated albumin stimulates TGF-β1 production and protein kinase C activity in glomerular endothelial cells. *Kidney Int* 59:673–681, 2001

50. Wolf G, Hamann A, Han DC, Helmchen U, Thaiss F, Ziyadeh FN, Stahl RA: Leptin stimulates proliferation and TGF-β expression in renal glomerular endothelial cells: potential role in glomerulosclerosis. *Kidney Int* 56:860–872, 1999